Complex Systems **10** (1996) 321–343

Self-similarity and Fine Structures in the Linear-logistic Map

B. L. Tan
T. T. Chia*
Department of Physics,
National University of Singapore,
Kent Ridge, Singapore 119260

Abstract. From the graphs of the Lyapunov exponent of the linear-logistic map, (which is linear in the region on the left of its maximum but logistic-like on its right), against its parameter r, the stable cycles within the chaotic region can be classified into six different patterns. In each of these patterns, at least one increasing arithmetic progression is present and decreasing arithmetic progressions may also be present as well; all the terms of these progressions are intermingled with chaos. One of these patterns is self-similar, while in another the period-adding phenomenon occurs. All the patterns are interrelated through their dependence on the same variables.

1. Introduction

One-dimensional maps, such as the symmetric logistic [1] and asymmetric maps [2–18, 29], have very interesting dynamical properties and are studied as possible prototypes of more complicated dynamical systems. Recently, the interest in asymmetric maps was enhanced by the discovery that the dynamical structures of some physical processes are similar to those of these simple maps [19–22]. One of these is a map that is quadratic at the right of its extremum but linear at the left [19, 20]. This can be described by the *linear-logistic map*:

$$g(x_n) = \begin{cases} 2rx_n & \text{if } x_n < 1/2 \\ 4rx_n(1-x_n) & \text{if } x_n \geq 1/2. \end{cases} \tag{1}$$

We have found that the manner in which period-doublings occur in this linear-logistic map is very unusual in two ways when compared to the logistic and other quadratic maps [16]. One is that it undergoes period-doublings whenever $dg^m(x)/dx$, the slope at any of its m stable fixed points, is -1 or

*Electronic mail address: `phyctt@leonis.nus.edu.sg`.

0. The other is that the rate of evolution of a new cycle, created by period-doubling bifurcation, into a superstable cycle and then to an unstable cycle, is very abrupt in the linear-logistic map.

In this paper we study the self-similarity and fine structures of the linear-logistic map numerically. In section 2, we use the variation of the Lyapunov exponent λ with the parameter r as a means for classifying the stable orbits of the linear-logistic map. From the graphs of λ versus r in the chaotic region, we can identify periodic windows possessing many interesting fine structures. We then classify the periods of some of the stable cycles in these fine structures into six different patterns. Each pattern consists of at least an increasing arithmetic progression (AP) which may or may not be accompanied by one or more decreasing APs. For each pattern, a general expression for each of the terms and several numerical examples are given.

We find that the first pattern studied is self-similar while in the last pattern, the phenomenon of period-adding occurs. All the patterns are found to occur on different scales, meaning that they are present in enlarged regions of the r-λ plane. Further, all these patterns are interrelated as they are dependent on the same variables n and p which will be defined below. It is interesting that one of these patterns has already been observed experimentally [20].

2. Study of fine structures using the Lyapunov exponent

The linear-logistic map has very rich fine structures as many periodic windows exist in the chaotic region. For quantification of chaos and order, the Lyapunov exponent

$$\lambda = \lim_{N\to\infty} \frac{1}{N} \sum_{i=0}^{N-1} \ln |g'(x_i)| \tag{2}$$

is often used. When $\lambda < 0$, the orbits are periodic and stable; when $\lambda > 0$, they are chaotic or unstable. In addition, λ is 0 at all period-doubling bifurcation and tangent bifurcation points, and at all accumulation points of the period-doubling cascades. Thus from the graphs of λ as a function of r, unstable periodic and chaotic orbits can be distinguished from stable periodic ones and some of the bifurcation points identified.

As our map is not differentiable at the extremum, the usual derivative in the above definition of λ should be replaced by

$$g'(x_i) = \frac{ag'(x_i+\epsilon) + bg'(x_i-\epsilon)}{a+b} \tag{3}$$

where a and b are two real numbers and ϵ is an infinitesimal. Clearly, this definition reduces to the usual one for maps which are differentiable everywhere.

As the measure of the extremum point is zero for our map, the probability of any iterate x_i being equal to the extremum value is zero in view of the finite precision of computer arithmetic. Hence, though the formal definition of λ given in equation (2) fails at the extremum point, in practice, this failure is

not realized. The usual derivative at the extremum point $x = 1/2$ (obtained by formally differentiating the function defined at this point) gives 0 implying that λ is equal to minus infinity should any one of the iterates x_i be equal to $1/2$. In all our calculations, we find that λ is always finite which means that equation (2) with the usual definition of the derivative can be used.

Here we use the r-λ graphs to classify the stable orbits. From special features of the stable cycles in the chaotic regions of these graphs, we can identify sets of stable cycles with periods that can be conveniently classified into different patterns with explicitly defined rules, which shall be elaborated below. An initial value $x_0 = 0.1$ is used in all our computations.

2.1 Pattern I

When λ is plotted against r, we find that there exist many periodic windows which, together with the periodic region before the onset of chaos, are referred to simply as *periodic regions*. We find that every region consists of several periodic subregions over each of which the period is constant. The most obvious pattern observed, which we call Pattern I, is shown in Figure 1(a). The subregions relevant to this pattern are indicated by numbers representing the periods of the corresponding stable cycles. Here, in the subregion labeled '2' (appearing on the extreme left portion of the graph), λ decreases from zero to a negative number while in each of the rest of the labeled subregions which have structurally the same features in the r-λ plane, λ increases monotonically from a negative number to zero. For example, in the subregion labeled '4' shown in Figure 1(a), where r ranges from about 0.809 to about 0.819 and λ from about -4.0 to 0, there are stable cycles with period 4. From Figure 1(a), we see that the periods of the stable cycles in these labeled subregions of Pattern I form an AP

$$p \to 2p \to 3p \to 4p \to 5p \to \cdots$$

with a common difference $\Delta = p = 2$. We expect that an infinite number of terms in the sequence should exist, though of course, this cannot be observed in practice due to the finite precision of computers and the decreasing size of the subregions with increasing r.

The transition from the period 2 subregion to the period 4 subregion is to be contrasted with that in the logistic map. In the latter, transition from one period to another always occurs after λ has reached a value of 0. Here there is a transition in period from the period 2 subregion to the period 4 subregion even though λ never reaches 0. This sudden transition is in agreement with the earlier result in [16] showing that an infinitesimal increase in r causes the superstable 2-cycle to bifurcate to a superstable 4-cycle.

As r increases the 4-cycle period-doubles into an 8-cycle when $\lambda = 0$, a process similar to that of the logistic map. Subsequently, this 8-cycle is observed to bifurcate (by an unusual period-doubling mentioned earlier) into a 16-cycle at a nonzero value of λ in a manner similar to the transition of period 2 into period 4. This 16-cycle is now observed to bifurcate into a

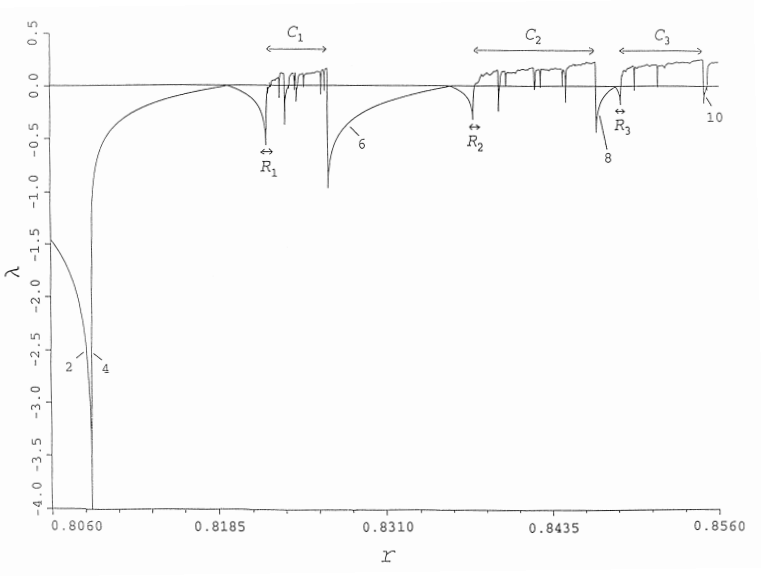

(a)

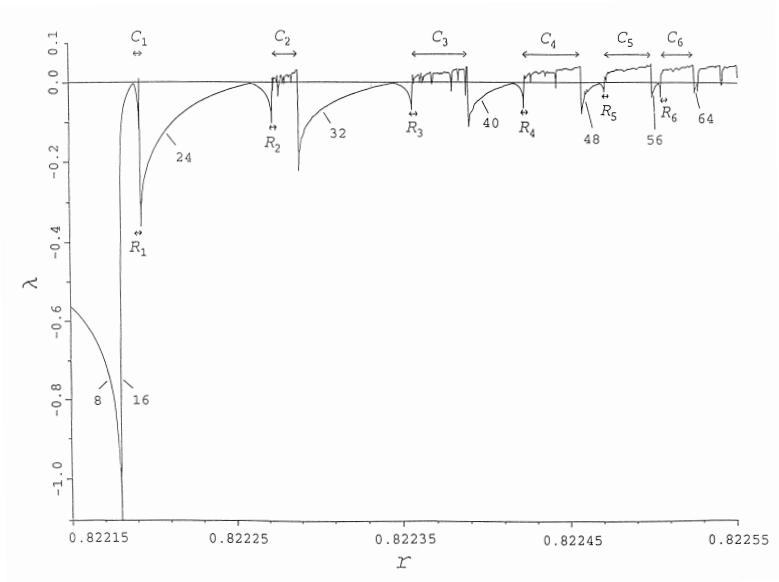

(b)

Figure 1: (a) Lyapunov exponent λ as a function of r showing Pattern I with $p = 2$. (b) Enlargement of a small region R_1 in (a), showing Pattern I with $p = 8$. Note that the two figures are self-similar.

32-cycle when $\lambda = 0$ and so on. Though we can only see a few of such period-doublings before the first entrance into chaos, there should exist an infinite number of them as higher-order cycles occupy very narrow intervals and thus are not visible from the graph.

We find that Pattern I is self-similar at smaller length scales. Figure 1(b) is the enlargement of the small region labeled R_1 in Figure 1(a) with r ranging from 0.82215 to 0.82255. The labeled subregions of Figure 1(b) obey a pattern similar to that of Figure 1(a) with the value of the common difference Δ of this AP equal to $p = 8$. Both figures show self-similar structures. As r increases, the periodic windows of higher terms become narrower. Pattern I can also be observed from the enlargement of other portions of both these figures, say, regions R_2 and R_3 of Figure 1(a) or region R_1 of Figure 1(b). In these three enlarged regions, the series are $12 \to 24 \to 36 \to 48 \to 60 \to \cdots$, $16 \to 32 \to 48 \to 64 \to 80 \to \cdots$, and $32 \to 64 \to 96 \to 128 \to 160 \to \cdots$ with $\Delta = 12$, 16, and 32 respectively.

From measurements of the intensity of pulses in a laser cavity [20], it was found that these pulse intensities obey an equation "where the maximum is quadratic at right but linear at left," that is, by an equation of the same form as the linear-logistic map. The discovery of several mathematical series is reported in [20]. In fact, what was observed are those prominent periodic regions in our Figure 1(a) and enlargements of regions R_1, R_2, and R_3 of the same figure. However, it was not mentioned that the terms of the series actually formed APs as some of these terms were probably not observed. Hence, our Pattern I accounts for their experimental observations.

One characteristic feature of Pattern I is the occurrence of chaos between all the terms of the sequence, except between the first and second terms. Within each of the chaotic regions lying between two consecutive terms, there are tiny periodic windows which can be classified into other patterns, as we show later.

2.2 Pattern II

With the exception of the first term, all the other terms of Pattern I are separated by chaotic regions; the first chaotic region is denoted by C_1, the second by C_2, and so on, as illustrated in Figure 1. Within each C_n, where $n = 1, 2, 3, 4, 5, \ldots$, we can find stable cycles with n different periods which form a finite AP consisting of n terms and having a common difference $\Delta = p$. We refer to this structure as Pattern II. Surprisingly, the number of terms within C_n is equal to n, the subscript of C_n.

Figure 2(a) shows a schematic diagram of the general Pattern I with terms $p, 2p, 3p, 4p, 5p, 6p, \ldots$ separated by the chaotic regions C_n. The same figure also shows that within each C_n there exists Pattern II consisting of structurally similar terms. (A scaled diagram of Pattern II is shown in Figure 2(b).) The periods of cycles relevant to Pattern I and Pattern II are labeled in the diagram with the terms of Pattern II underlined. Here p is an integer which, in the case of Pattern I of Figure 1(a), is 2. For simplicity, we only

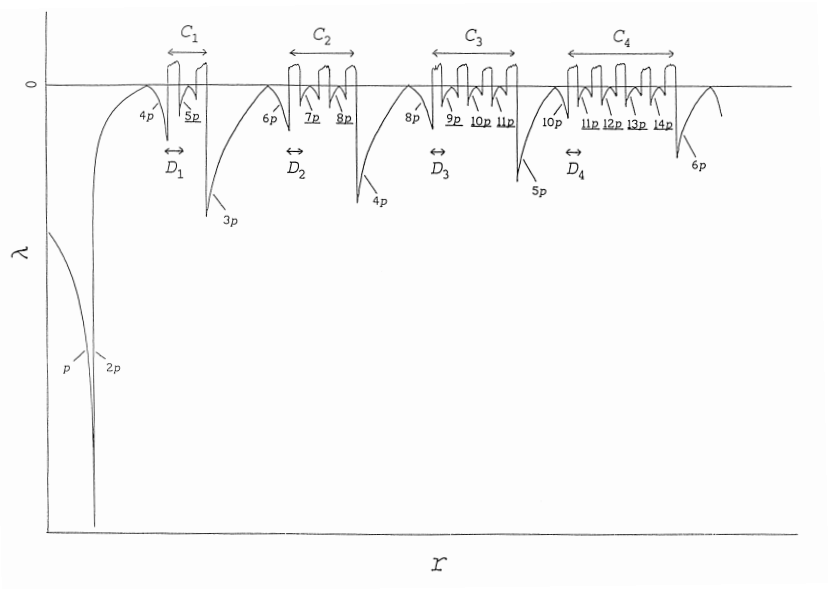

(a)

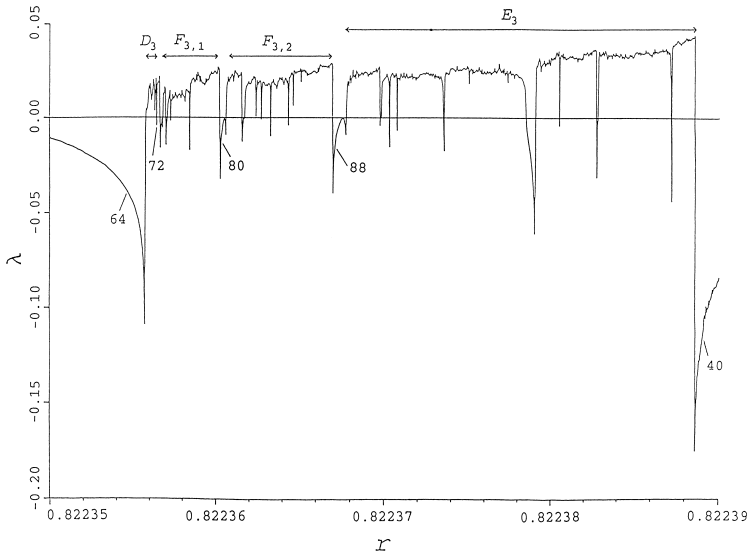

(b)

Figure 2: (a) Schematic diagram of Pattern I, with Pattern II embedded within C_n (see Figure 1 for region C_n). The terms belonging to Pattern II are underlined. (b) An example of Pattern II occurring within region C_3 of Figure 1(b).

Table 1: The terms of Pattern II for the labeled regions C_1 to C_3 in Figure 1(a) with $p = 2$, and the labeled regions C_1 to C_6 in Figure 1(b) with $p = 8$.

	Region	Terms of Pattern II
(i) From Figure 1(a):	C_1	10
	C_2	14, 16
	C_3	18, 20, 22
(ii) From Figure 1(b):	C_1	40
	C_2	56, 64
	C_3	72, 80, 88
	C_4	88, 96, 104, 112
	C_5	104, 112, 120, 128, 136
	C_6	120, 128, 136, 144, 152, 160

show the periodic windows relevant to Pattern II in C_n, though there exist many more periodic windows which may occupy a great portion of C_n and which may appear structurally similar to the terms of Patterns I or II. These other windows are found to belong to other patterns described below. We present the schematic diagram first instead of a scaled diagram as the latter cannot display this information as well, since the terms of Pattern II occupy much smaller intervals than those of Pattern I.

It can be seen in Figure 2(a) that the first term of Pattern II in C_n is formed by adding p to the period-doubled term of Pattern I which lies just before C_n. The other terms of this Pattern II are, of course, obtained from the first term by adding p successively since this pattern forms an AP. Hence we can easily predict all the terms of Pattern II belonging to any C_n. In particular, C_1 contains only one term that is always given by $4p + p$ or $5p$. In general, the tth term of Pattern II in C_n is given by $(2n + 2 + t)p$ where $t = 1, 2, 3, \ldots, n$. Thus the terms in C_n range from $(2n + 3)p$ to $(3n + 2)p$ in steps of p. As an illustration, Table 1 shows these terms of Pattern II for the labeled regions C_1 to C_3 of Figure 1(a) where $p = 2$, as well as those terms of regions C_1 to C_6 in Figure 1(b) where $p = 8$. We have actually verified that all these terms do exist, and have further verified the existence of Pattern II in other parameter ranges, such as those falling within the regions labeled R_2 and R_3 of Figure 1(a) and regions R_1 to R_6 of Figure 1(b) in each of which the values of p are different.

A scaled diagram of Pattern II is given in Figure 2(b), an enlargement of region C_3 in Figure 1(b), where the terms 72, 80, and 88 that make up Pattern II are indicated. Here, there are many chaotic regions that together occupy a larger portion of the C_3 region than for the previously discussed terms. Thus, it requires some effort to isolate these terms especially when they occupy such small intervals of r that on the same scale they do not appear to resemble those more prominent terms which occupy larger intervals, though on a smaller scale they would.

2.3 Pattern III

In Figure 2(a) the beginning portion of each C_n region, sandwiched between the first term of Pattern II and the period-doubled term of Pattern I just before C_n, is labeled D_n. Note that a D_n region always exists within any C_n region of any scale, for example, those appearing in Figure 1. From an enlargement of any one of these D_n regions, we observe that many of the stable cycles lying within it have periods that fall into a certain pattern which we refer to as Pattern III.

The region D_n consists of n basic blocks that form Pattern III. Note that, interestingly, the number of such basic blocks is the same as the subscript of the region C_n. This is shown schematically in Figure 3(a). Within the ith block, where $i = 1, 2, 3, \ldots, n$, we observe that at the beginning of this block, some of the stable cycles with the same structural features, have even periods that form an increasing AP

$$\begin{aligned}&[6N-(i-1)]p \to [8N-(i-1)]p \to [10N-(i-1)]p \\ &\quad \to [12N-(i-1)]p \to [14N-(i-1)]p \to \cdots\end{aligned}$$

as r is increased. This series has a common difference of $2Np$ where $N = n+1$ (to be deduced below) and p is the common difference of Pattern I. At some value of r, this series gives way to a decreasing AP consisting of the following terms

$$\begin{aligned}&\cdots \to [11N-(i-1)]p \to [9N-(i-1)]p \to [7N-(i-1)]p \\ &\quad \to [5N-(i-1)]p \to [3N-(i-1)]p\end{aligned}$$

with the same common difference $|\Delta| = 2Np$ where N and p have been defined above. Note again that these terms are also structurally similar to each other. For example, in block 1 as r increases, the following increasing AP

$$6Np \to 8Np \to 10Np \to 12Np \to 14Np \to \cdots$$

develops from the beginning of the block. This is followed by a decreasing AP

$$\cdots \to 11Np \to 9Np \to 7Np \to 5Np \to 3Np.$$

We find that for all values of n, it is easier to locate the terms of the ith block in region D_n than in region D_{n+1}. Within each region D_n, the interval of r occupied by the ith block decreases with increasing i. Further, within any of these blocks the higher terms of both increasing and decreasing APs tend to occupy narrower intervals. This observation implies that there should exist an infinite number of terms, though of course this cannot be proven numerically.

From a λ versus r graph, we can easily distinguish pictorially the terms of the increasing AP from that of the decreasing AP of Pattern III: the terms of an increasing AP form the rising portions of the "mountains," whereas

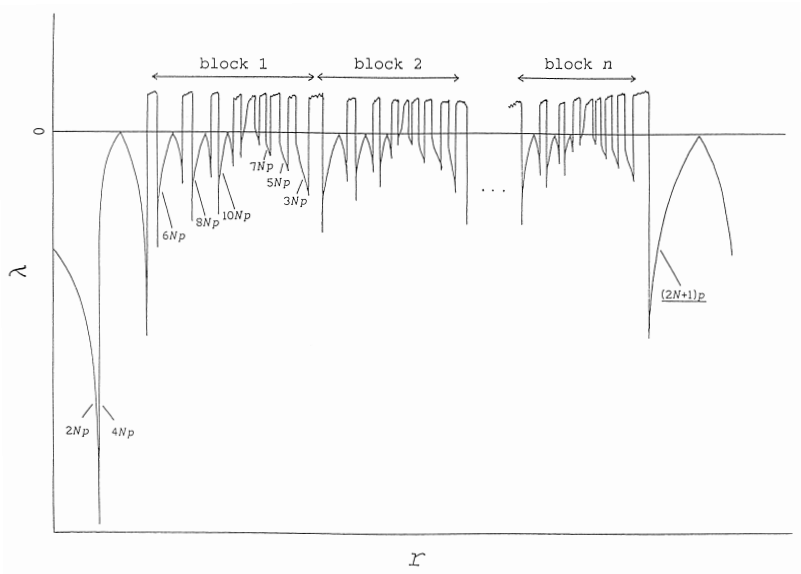

(a)

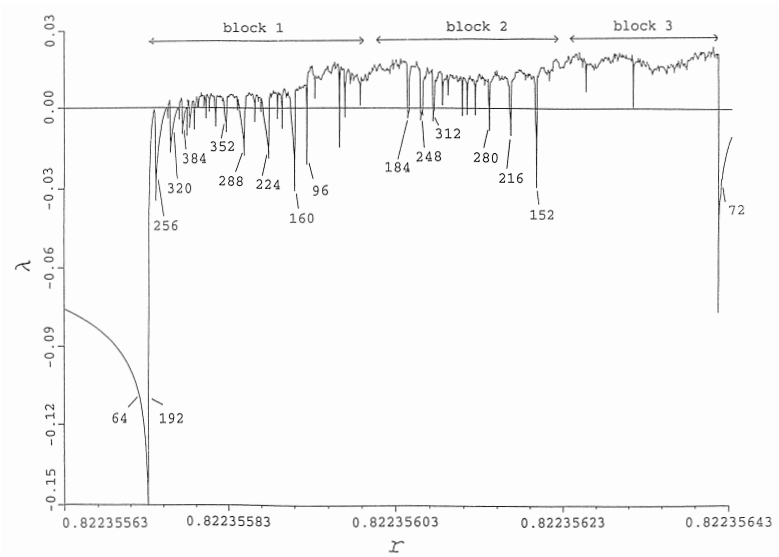

(b)

Figure 3: (a) Schematic diagram of Pattern III, which occurs in D_n (see Figure 2(a) for region D_n). The terms in each block i, where $i = 1, 2, 3, \ldots, n$, are given in the text. (b) An example of Pattern III occurring within region D_3 of Figure 2(b).

those of a decreasing AP form the descending portions of "valleys," as can be seen in Figure 3(a). This pictorial rule also applies to other patterns to be presented below as well as to Patterns I and II: this is not too surprising as the terms of each AP of each pattern must be structurally similar to each other. Note that only mountains are present in Figures 1 and 2 as the terms of Patterns I and II form increasing APs.

From Figures 2(a) and 3(a), it can be deduced that $N = n + 1$ and that $2N = 4, 6, 8, 10, 12, \ldots$ for the D_n region where $n = 1, 2, 3, 4, 5, \ldots$ respectively. If Pattern III in Figure 3(a) is examined carefully, it can be seen that the first half of block 1, where mountains are formed, together with the two terms $2Np$ and $4Np$ just before it, are actually Pattern I if $2Np$ is replaced by p.

The first numerical example of Pattern III is obtained from an enlargement of region D_1 (though not indicated) of Figure 1(a), where $p = 2$. As $n = 1$, then according to Figure 3(a), D_1 must lie within the terms $2Np$ or 8 and $(2N + 1)p$ or 10. Thus D_1 overlaps the entire region R_1 in Figure 1(a) (which forms Pattern I) and extends into the only term of Pattern II in C_1, which is 10. We observe in D_1 the increasing AP

$$8 \to 16 \to 24 \to 32 \to 40 \to 48 \to \cdots$$

followed by the decreasing AP

$$\cdots \to 52 \to 44 \to 36 \to 28 \to 20 \to 12$$

with $|\Delta| = 2Np = 8$ for each AP.

Another example is given by region D_3, which forms part of C_3, in Figure 1(b) which is an enlargement of the small region R_1 of Figure 1(a). Here, as indicated in the diagram, $p = 8$ and $N = n + 1 = 4$. Thus region D_3 must lie between the term $2Np$ or 64 and the term $(2N + 1)p$ or 72 and this is indicated in Figure 2(b). As $n = 3$, there exist three blocks where the terms are given by

$$192 \to 256 \to 320 \to 384 \to 448 \to 512 \to \cdots$$
$$\cdots \to 416 \to 352 \to 288 \to 224 \to 160 \to 96$$

for block 1,

$$184 \to 248 \to 312 \to 376 \to 440 \to 504 \to \cdots$$
$$\cdots \to 408 \to 344 \to 280 \to 216 \to 152 \to 88$$

for block 2, and

$$176 \to 240 \to 304 \to 368 \to 432 \to 496 \to \cdots$$
$$\cdots \to 400 \to 336 \to 272 \to 208 \to 144 \to 80$$

for block 3. Thus within each block, there exists an increasing AP followed by a decreasing AP where $|\Delta| = 2Np = 64$ for each AP.

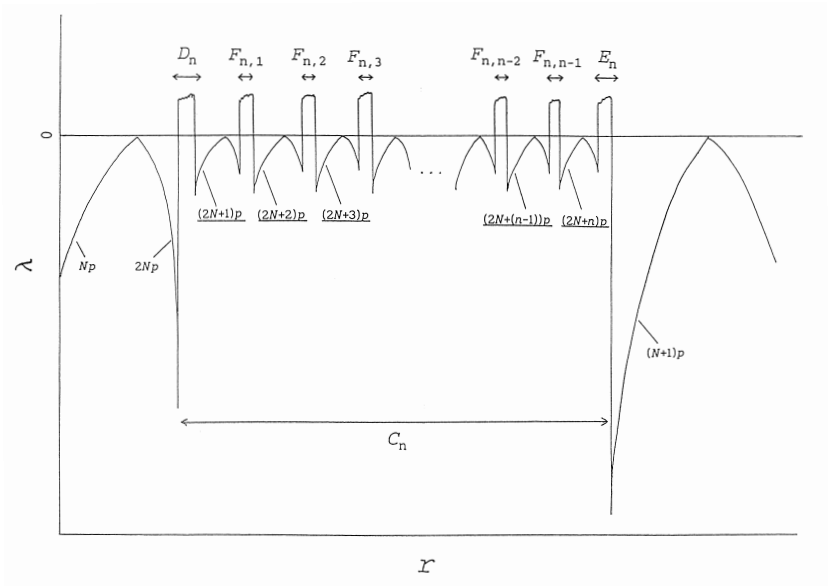

Figure 4: Schematic diagram of Pattern II in C_n, with the terms expressed as a function of N. Also shown are the locations of regions D_n, E_n, and $F_{n,m}$, where $1 \leq m \leq n-1$.

A scaled diagram of Pattern III discussed in the preceding example is given in Figure 3(b), which shows an enlargement of region D_3 from Figure 2(b) with some of the terms making up this pattern for block 1 and block 2 labeled. Other terms given in the preceding numerical example are not visible in this graph as they occupy very narrow intervals.

2.4 Pattern IV

The terms of the general Pattern II appearing in region C_n can be expressed as functions of N and are shown underlined in Figure 4 to distinguish them from the two terms of Pattern I and a period-doubled term which are also shown. All the terms except Np are separated from each other by chaotic regions labeled D_n, $F_{n,1}$, $F_{n,2}$, $F_{n,3}, \ldots, F_{n,n-2}$, $F_{n,n-1}$, and E_n in order of increasing r in the same figure.

Just as some of the stable cycles within the chaotic region D_n can be arranged into Pattern III, it can be seen that another interesting pattern, called Pattern IV, exists within region E_n which lies between the last term of Pattern II and the next nearest term of Pattern I, that is, between the terms $(2N+n)p$ and $(N+1)p$ shown in Figure 4.

Figure 5(a) shows a schematic diagram of Pattern IV occurring in region E_n with the terms of this pattern expressed as functions of n, N, and p which are the same variables defined earlier. We observe that as r is increased up

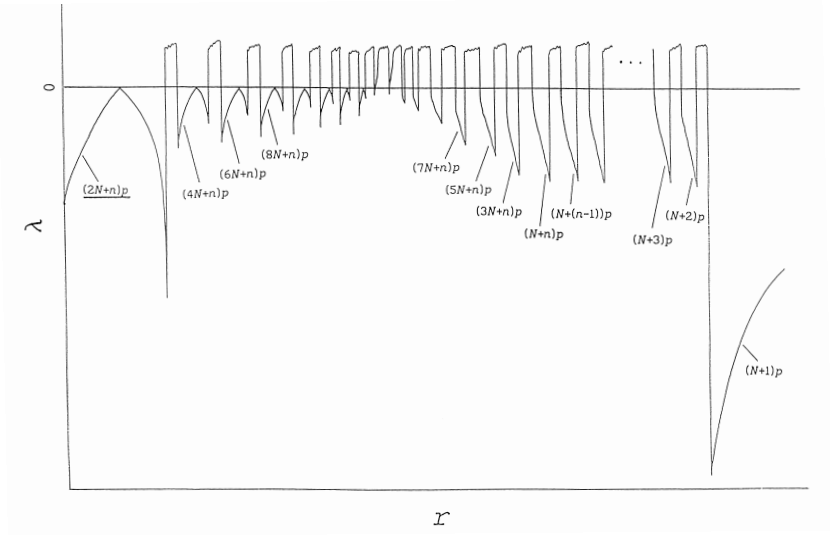

(a)

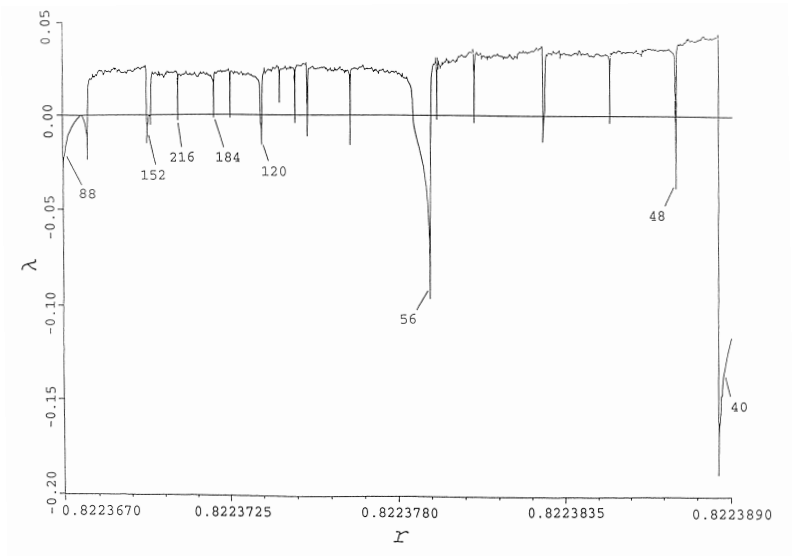

(b)

Figure 5: (a) Schematic diagram of Pattern IV, which occurs in E_n (see Figure 4 for region E_n). (b) An example of Pattern IV occurring within region E_3 of Figure 2(b).

to a certain value, the stable cycles in this region have periods which form an increasing AP

$$(4N+n)p \to (6N+n)p \to (8N+n)p \to (10N+n)p \\ \to (12N+n)p \to \cdots$$

with a common difference $\Delta = 2Np$. Note that the term $(2N+n)p$ belonging to Pattern II just before region E_n can also be regarded as the first term of this increasing AP. When r increases beyond this value, the periods fall into a decreasing AP with $|\Delta| = 2Np$:

$$\cdots \to (9N+n)p \to (7N+n)p \to (5N+n)p \\ \to (3N+n)p \to (N+n)p.$$

This decreasing AP terminates at $(N+n)p$ which in turn is followed by another decreasing AP consisting of n terms with $|\Delta| = p$:

$$(N+n)p \to \cdots \to (N+5)p \to (N+4)p \to (N+3)p \\ \to (N+2)p \to (N+1)p.$$

The term $(N+n)p$ is regarded as belonging to both decreasing APs and that when $n = 1$, the last series does not exist as it has only one term. As higher terms usually occupy narrower intervals of r, we expect that in both of the first two APs, each with $|\Delta| = 2Np$, there should exist an infinite number of terms. It should be noted that all the terms belonging to the same AP of Pattern IV have similar features in the r-λ plane.

When the region C_1 shown in Figure 1(a) is enlarged (which is not shown here), we find that within the region E_1 there exists an example of Pattern IV with $n = 1, N = 2$, and $p = 2$. We observe an increasing AP followed by only one decreasing AP in E_1, with $|\Delta| = 2Np = 8$ for both APs:

$$10 \to 18 \to 26 \to 34 \to 42 \to 50 \to \cdots \\ \cdots \to 46 \to 38 \to 30 \to 22 \to 14 \to 6.$$

If $n > 1$, an extra decreasing AP exists with $|\Delta| = p$ having n terms. For instance, there exists one increasing and two decreasing APs in the region E_3 which forms part of C_3 in Figure 1(b) where $p = 8$, $n = 3$, and $N = 4$. This region, which occurs between the terms $(2N+n)p = 88$ and $(N+1)p = 40$, is indicated in Figure 2(b) and an enlargement of E_3 is shown in Figure 5(b). We observe in E_3 another example of Pattern IV consisting of the following three APs:

$$88 \to 152 \to 216 \to 280 \to 344 \to 408 \to \cdots \\ \cdots \to 376 \to 312 \to 248 \to 184 \to 120 \to \underline{56} \to \underline{48} \to \underline{40}$$

with the three underlined terms forming the $n = 3$ terms of the last decreasing AP with $|\Delta| = p = 8$, while $|\Delta| = 2Np = 64$ for each of the other two preceding APs.

2.5 Pattern V

Between any two consecutive terms of the n terms of Pattern II occurring within C_n as shown in Figure 4, there exists another chaotic region labeled $F_{n,m}$ where the first subscript refers to the region C_n while the second can range from 1 to $n-1$. When we enlarge any one of these $F_{n,m}$ regions which lie between the terms $(2N+m)p$ and $(2N+(m+1))p$ where $1 \leq m \leq n-1$ and as before, $N = n+1$, we find an interesting variation of λ with r as shown schematically in Figure 6(a). In each of these $(n-1)F_{n,m}$ regions, there are stable cycles with periods that obey a pattern, referred to as Pattern V. Clearly, the $F_{n,m}$ regions are present only if n is greater than 1.

In each of the regions $F_{n,m}$, there exist a finite number of blocks and, surprisingly, this number is exactly equal to n. Within each of these n blocks, labeled block i in Figure 6(a) where $i = 1, 2, 3, \ldots, n$, there are stable cycles with periods that fall into an increasing AP for values of r less than a certain value and into a decreasing AP for larger values of r. This increasing AP takes the form

$$[4N + (m-(i-1))]p \to [6N + (m-(i-1))]p \to [8N + (m-(i-1))]p$$
$$\to [10N + (m-(i-1))]p \to [12N + (m-(i-1))]p \to \cdots$$

with a common difference $\Delta = 2Np$ while the decreasing AP is

$$\cdots \to [11N + (m-(i-1))]p \to [9N + (m-(i-1))]p$$
$$\to [7N + (m-(i-1))]p \to [5N + (m-(i-1))]p \to [3N + (m-(i-1))]p$$

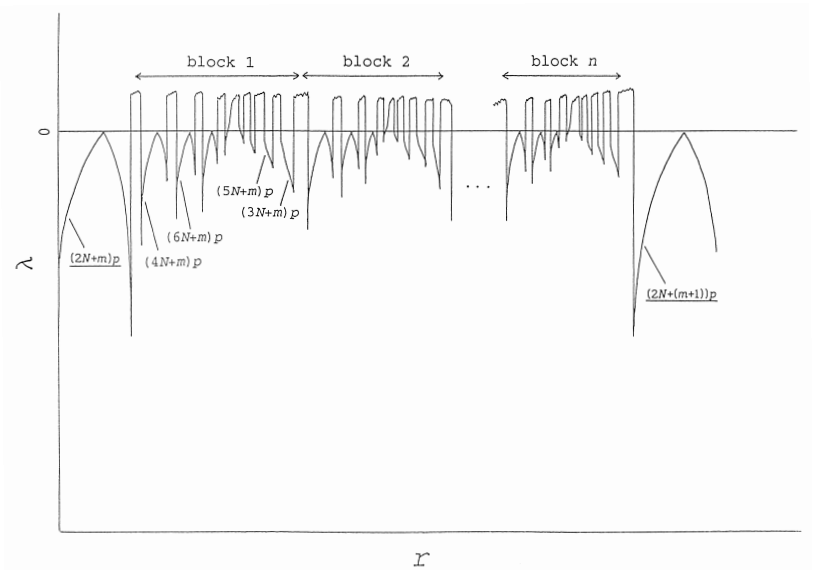

(a)

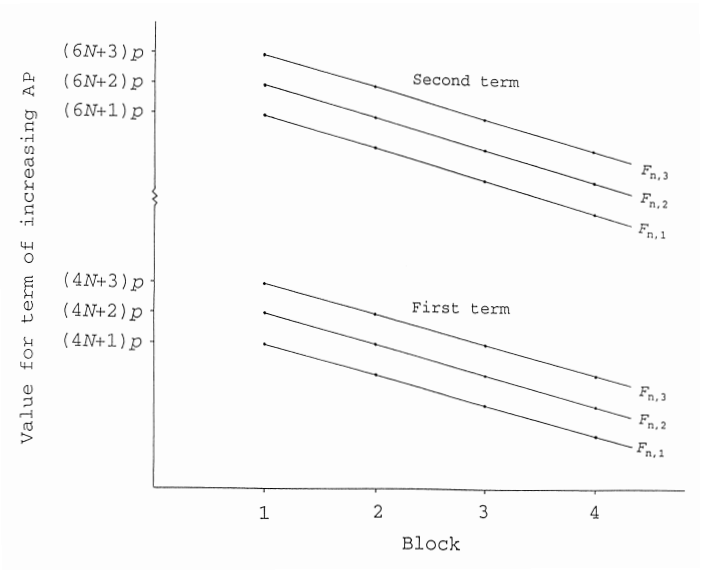

(b)

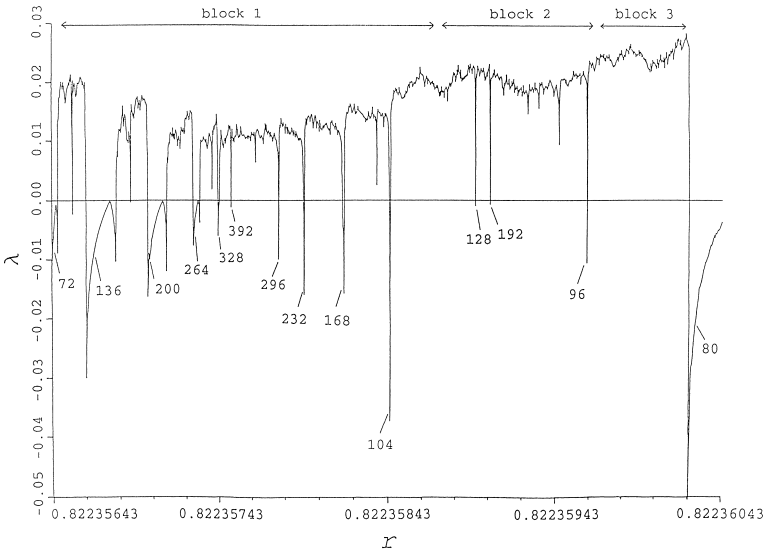

(c)

Figure 6: (a) Schematic diagram of Pattern V, which occurs in the region $F_{n,m}$ between any two consecutive terms of Pattern II in C_n, where $n \geq 2$. See the text for the terms in each block i, where $i = 1, 2, 3, \ldots, n$. (b) Schematic diagram showing the values of the first and second term of each increasing AP of Pattern V found in block i, region $F_{n,m}$ as a function of i but for a fixed n. (c) An example of Pattern V occurring in the region $F_{3,1}$ between the consecutive terms 72 and 80 of Figure 2(b).

which again has $|\Delta| = 2Np$. Within each block, the higher terms usually occupy narrower intervals of r and therefore, each AP should contain an infinite number of terms. We find that within any $F_{n,m}$ region inside the C_n region, the interval of r occupied by the ith block decreases with increasing i and that it is easier to identify Pattern V for smaller values of m. Further, it is easiest to recognize Pattern V within C_n when n is smaller.

For a fixed n, Figure 6(b) shows schematically the first and second terms of each increasing AP of Pattern V, found within block i of region $F_{n,m}$, as a function of i. It is obvious that the higher terms are located on loci parallel to those shown but shifted upwards by a multiple of $2Np$. Hence, it can be deduced that in a given $F_{n,m}$ region, each term of the increasing AP decreases by p as a higher block is reached. Moreover, within the same block and the same $F_{n,m}$ region, successive terms differ by $2Np$.

The first example of Pattern V is found within $F_{2,1}$ lying inside region C_2 of Figure 1(b). Here $n = 2$, $N = 3$, $m = 1$, and $p = 8$. Table 1 shows that Pattern II occurring within C_2 has only two terms, 56 and 64. Thus, there exists only one $F_{2,m}$ region in C_2, namely $F_{2,1}$. Further, as $n = 2$, Pattern V occurring within this $F_{2,1}$ region consists of only two blocks in each of which there is an increasing AP followed by a decreasing AP each with $|\Delta| = 2Np = 48$. The terms of block 1 and block 2 are given by

$$104 \to 152 \to 200 \to 248 \to 296 \to 344 \to \cdots$$
$$\cdots \to 320 \to 272 \to 224 \to 176 \to 128 \to 80$$

and

$$96 \to 144 \to 192 \to 240 \to 288 \to 336 \to \cdots$$
$$\cdots \to 312 \to 264 \to 216 \to 168 \to 120 \to 72$$

respectively.

Another example of Pattern V occurs within the region $F_{3,1}$, the first of the two $F_{3,m}$ regions lying within region C_3 shown in Figure 1(b). Here $n = 3$, $N = 4$, $m = 1$, and $p = 8$. Note that the terms of Pattern II on either side of $F_{3,1}$ are equal to 72 and 80 which are given by $(2N + 1)p$ and $(2N + 2)p$ respectively and in Table 1. Within this $F_{3,1}$ region, as $n = 3$, we observe Pattern V which contains three blocks with terms given by

$$136 \to 200 \to 264 \to 328 \to 392 \to 456 \to \cdots$$
$$\cdots \to 424 \to 360 \to 296 \to 232 \to 168 \to 104$$

for block 1,

$$128 \to 192 \to 256 \to 320 \to 384 \to 448 \to \cdots$$
$$\cdots \to 416 \to 352 \to 288 \to 224 \to 160 \to 96$$

for block 2, and

$$120 \to 184 \to 248 \to 312 \to 376 \to 440 \to \cdots$$
$$\cdots \to 408 \to 344 \to 280 \to 216 \to 152 \to 88$$

for block 3. In each case, we observe an increasing AP followed by a decreasing AP each with $|\Delta| = 2Np = 64$.

Figure 6(c) is a scaled diagram showing Pattern V of the preceding example. This figure is an enlargement of the $F_{3,1}$ region lying between the two terms labeled 72 and 80 shown in Figure 2(b). It should be noted that as some of the terms of Pattern V occupy very small intervals of r, they are not visible on the graph.

2.6 Pattern VI

In this section we encounter the phenomenon of period-adding in another pattern of the linear-logistic map. Period-addings have already been observed experimentally [23] and in other maps [24–28]. Though in some sense it resembles the summation rule for discontinuous maps [14, 15], to our knowledge, this is the first time that period-addings have been observed in a continuous, one-dimensional map without a cusp [26–28].

When certain regions of Patterns III, IV, and V are enlarged, we find the existence of yet another pattern, called Pattern VI. Surprisingly, this last pattern has the same structure whether it orginates within Pattern III, IV, or V.

We have shown that both Patterns III and V contain blocks, each of which contains an increasing AP and a decreasing AP with common differences $|\Delta| = 2Np$. Pattern IV consists of an increasing AP and a decreasing AP with the same $|\Delta| = 2Np$ and another decreasing AP with a different $|\Delta| = p$ if $N > 2$. When we enlarge the region between any two consecutive terms of any of these decreasing APs with $|\Delta| = 2Np$ (i.e., the region between two consecutive valleys, shown in Figures 3(a), 5(a), and 6(a) which correspond respectively to Patterns III, IV, and V), we find the existence of many new prominent stable cycles with periods that can be arranged into Pattern VI. An enlargement of this region is shown schematically in Figure 7(a).

In Figure 7(a), it can be seen that Pattern VI consists of two parts. In part (i), we observe a series of mountains followed by a series of valleys with the mountain terms forming an increasing AP and the valley terms forming a decreasing AP just as in Patterns III through V. In part (ii) of Pattern VI, the terms have valley-like appearance but unlike the earlier valleys, these new terms form an *increasing* AP instead. Further, we find that in this part, the terms obey a period-adding rule which will be elaborated below. It is interesting to note that the presence of either an increasing AP (as in Patterns I through V and part (i) of Pattern VI) or an AP with terms which have valley-like structures in the r-λ plane (as in Patterns III through V and part (i) of Pattern VI) does not guarantee the existence of period-adding whereas in part (ii) of Pattern VI, period-adding occurs in an increasing AP consisting of terms with valley-like appearance.

Whenever Pattern VI originates between two consecutive valleys of Pattern III with terms denoted by A and B, we observe in this pattern an increasing AP

$$A + 2Np \to A + 4Np \to A + 6Np \to A + 8Np \to A + 10Np \to \cdots$$

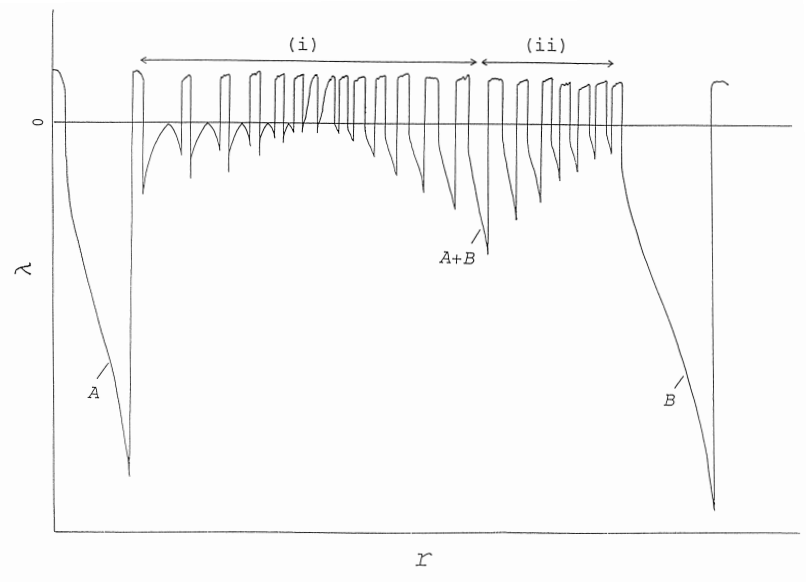

(a)

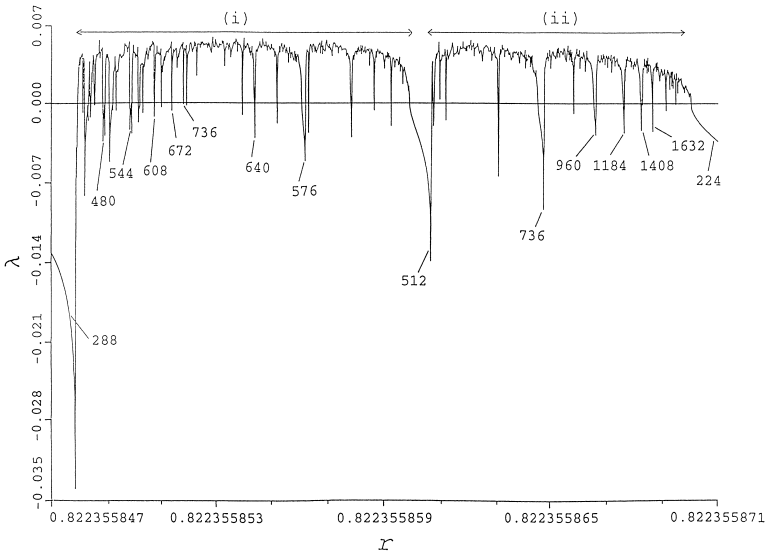

(b)

Figure 7: (a) Schematic diagram of Pattern VI, which occurs in the region between any two consecutive terms of the decreasing AP with $|\Delta| = 2Np$ belonging to Pattern III, IV, or V. See Table 2 for the values of A and B, as well as the sequences occurring in parts (i) and (ii). (b) An example of Pattern VI occurring in the region between the consecutive terms 288 and 224 of the decreasing AP of Pattern III, block 1 in Figure 3(b).

in the earlier segment of part (i). This is followed in the later segment by a decreasing AP

$$\cdots \to A + B + 8Np \to A + B + 6Np \to A + B + 4Np \\ \to A + B + 2Np \to A + B.$$

Each of these sequences has a common difference $|\Delta| = 2Np$.

Whenever Pattern VI originates from the region between two consecutive valleys of Pattern IV or Pattern V, again denoted by A and B, the increasing AP in part (i) of this pattern becomes

$$A + np \to A + (n + 2N)p \to A + (n + 4N)p \to A + (n + 6N)p \\ \to A + (n + 8N)p \to \cdots$$

while the decreasing AP in the same part has the same form as that originating from within Pattern III. Again, both APs have the same $|\Delta|$ of $2Np$. For Patterns III and V, we have only verified our results for block 1 since the other blocks have very narrow ranges in r.

In part (ii) of Pattern VI, regardless of whether it originates from consecutive valleys A and B of Pattern III, IV, or V, we always observe an increasing AP

$$A + B \to A + 2B \to A + 3B \to A + 4B \to A + 5B \to \cdots$$

with $\Delta = B$. This period-adding sequence is formed by just adding B to A repeatedly. Though this is an AP, it is not a special case of the previous sequences since here Δ is exactly equal to B, which is the term of the valley to the right of the sequence, whereas in the other sequences Δ is not related to any term on the right.

We expect that in each of the sequences discussed, an infinite number of terms should exist with the higher terms usually occupying narrower intervals.

As there are three possible ways in which Pattern VI can arise, namely from between two consecutive valleys of either Pattern III, IV, or V which all occur within C_n, the values of A and B which are the terms of these consecutive valleys will have different functional dependence on N, n, and m, as can be seen in Table 2. From the expressions for A and B, the precise forms of the increasing and decreasing APs of Pattern VI for each of the three cases can be easily obtained. These are also shown in Table 2.

We now give an explicit illustration for each of the three different ways Pattern VI can arise. Consider the first case when Pattern VI arises from between two consecutive valleys of the decreasing AP of block 1 within Pattern III, namely from the second example in section 2.3 where $p = 8$, $n = 3$, and $N = 4$. Here $A = 288$ and $B = 224$. From the expressions for A and B for case (a) shown in Table 2, we find that $s = 7$. Thus part (i) of Pattern VI consists of the increasing AP

$$352 \to 416 \to 480 \to 544 \to 608 \to 672 \to \cdots$$

Table 2: Values of A and B as well as the sequences occurring within parts (i) and (ii) of Pattern VI shown in Figure 7(a).

Details of Pattern VI	
Case (a):	Pattern VI originates from Pattern III, block 1
	$A = (s+2)Np$, $B = sNp$, possible values of $s = 3, 5, 7, 9, 11 \ldots$
	Part (i): $(s+4)Np \to (s+6)Np \to (s+8)Np \to (s+10)Np \to \cdots$ {increasing AP, $\Delta = 2Np$} $\cdots \to (2s+8)Np \to (2s+6)Np \to (2s+4)Np \to (2s+2)Np$ {decreasing AP, $\lvert\Delta\rvert = 2Np$}
	Part (ii): $(2s+2)Np \to (3s+2)Np \to (4s+2)Np \to (5s+2)Np \to \cdots$ {increasing AP, $\Delta = sNp$}
Case (b):	Pattern VI originates from Pattern IV
	$A = [(u+2)N+n]p, B = (uN+n)p, u = 1, 3, 5, 7, 9 \ldots$
	Part (i): $[(u+2)N+2n]p \to [(u+4)N+2n]p \to [(u+6)N+2n]p \to [(u+8)N+2n]p \to \cdots$ {increasing AP, $\Delta = 2Np$} $\cdots \to [(2u+8)N+2n]p \to [(2u+6)N+2n]p \to [(2u+4)N+2n]p \to [(2u+2)N+2n]p$ {decreasing AP, $\lvert\Delta\rvert = 2Np$}
	Part (ii): $[(2u+2)N+2n]p \to [(3u+2)N+3n]p \to [(4u+2)N+4n]p \to [(5u+2)N+5n]p \to \cdots$ {increasing AP, $\Delta = (uN+n)p$}
Case (c):	Pattern VI originates from Pattern V, block 1
	$A = [(v+2)N+m]p, B = (vN+m)p, v = 3, 5, 7, 9, 11 \ldots$
	Part (i): $[(v+2)N+2m]p \to [(v+4)N+2m]p \to [(v+6)N+2m]p \to [(v+8)N+2m]p \to \cdots$ {increasing AP, $\Delta = 2Np$} $\cdots \to [(2v+8)N+2m]p \to [(2v+6)N+2m]p \to [(2v+4)N+2m]p \to [(2v+2)N+2m]p$ {decreasing AP, $\lvert\Delta\rvert = 2Np$}
	Part (ii): $[(2v+2)N+2m]p \to [(3v+2)N+3m]p \to [(4v+2)N+4m]p \to [(5v+2)N+5m]p \to \cdots$ {increasing AP, $\Delta = (vN+m)p$}

which is followed by the decreasing AP

$$\cdots \to 832 \to 768 \to 704 \to 640 \to 576 \to 512.$$

Each of these two APs has $|\Delta| = 2Np = 64$. In part (ii) of Pattern VI, we have the period-adding sequence

$$512 \to 736 \to 960 \to 1184 \to 1408 \to 1632 \to \cdots$$

with $\Delta = B = 224$.

Figure 7(b) is a scaled portion of the r-λ plane showing the preceding example of Pattern VI. This figure is an enlargement of the region between the consecutive terms 288 and 224 of the decreasing AP occurring in block 1 of Figure 3(b). Some terms of the sequences of Pattern VI occupy very narrow intervals and are not visible in the graph.

The region between the valley terms $A = 120$ and $B = 56$ of the decreasing AP of the second example of Pattern IV presented in section 2.4 where $p = 8$, $n = 3$, and $N = 4$ gives rise to an example of Pattern VI. From the expressions for A and B for case (b), we find that $u = 1$. In part (i) of this Pattern VI we find an increasing and a decreasing AP, each with $|\Delta| = 2Np = 64$:

$$144 \to 208 \to 272 \to 336 \to 400 \to 464 \to \cdots$$
$$\cdots \to 496 \to 432 \to 368 \to 304 \to 240 \to 176.$$

In part (ii), we find the period-adding sequence

$$176 \to 232 \to 288 \to 344 \to 400 \to 456 \to \cdots$$

with $\Delta = B = 56$.

In the region between the two consecutive valley terms $A = 176$ and $B = 128$ of the decreasing AP of the first example of Pattern V given in section 2.5 where $p = 8$, $m = 1$, $n = 2$, and $N = 3$, we have an example of Pattern VI. From the expressions for A and B for case (c), we get $v = 5$. Part (i) of Pattern VI consists of the following increasing and decreasing APs:

$$192 \to 240 \to 288 \to 336 \to 384 \to 432 \to \cdots$$
$$\cdots \to 544 \to 496 \to 448 \to 400 \to 352 \to 304$$

each with $|\Delta| = 2Np = 48$, while part (ii) consists of the following period-adding sequence:

$$304 \to 432 \to 560 \to 688 \to 816 \to 944 \to \cdots$$

with $\Delta = B = 128$.

3. Conclusions and summary

From the graphs of the Lyapunov exponent λ against r, which are used as a means for classifying the stable orbits, we find many periodic windows in the chaotic region of the map with periodicities obeying some specified rules. We have classified some specific stable cycles in these windows into six different patterns and have formulated rules for the patterns. We find that Pattern I is self-similar as stable cycles in enlargements of the same diagram obey the same pattern (Figure 1). Both Patterns I and II are increasing APs. In each of Patterns III trhough VI, we find both increasing and decreasing APs. Though such APs have already been discovered to occur before the onset of chaos in one-dimensional discontinuous maps [4–7, 14, 15], these are different from those presented here. In our case, the terms of such APs occur after the onset of chaos and they are *always* interposed with chaos. Further, in Pattern VI, we find that the phenomenon of period-adding occurs. All these patterns, which are found to occur on different scales, are related to one another through their dependence on the same variables n and period

p. We can also use these patterns to predict the existence of certain stable cycles in some domains of r of the linear-logistic map.

A typical term in each AP of each of the above patterns can be expressed in terms of the integral variables such as n and p. Amazingly, these variables are intimately related to one another in different parts of the r-λ plane.

Though here we have identified six different patterns, obviously there exist many other very narrow periodic windows which remain to be classified and which may contain different patterns. However, it would be a formidable task to classify all these extremely narrow periodic windows.

It is amazing that, in the r-λ plane, this asymmetric linear-logistic map exhibits patterns that do not seem to exist in other known maps. We have found in an exploratory study that there is another map which seems to possess some of these patterns. This is the *logisitic-linear* map

$$j(x_n) = \begin{cases} 4rx_n(1-x_n) & \text{if } x_n \leq 1/2 \\ 2r(1-x_n) & \text{if } x_n > 1/2, \end{cases} \tag{4}$$

which is the mirror-image of the linear-logistic map.

Acknowledgment

This work was supported in part by the National University of Singapore.

References

[1] M. J. Feigenbaum, *Journal of Statistical Physics*, **19** (1978) 25.

[2] A. Arneodo, P. Coullet, and C. Tresser, *Physics Letters*, **70A** (1979) 74.

[3] H. Kawai and S. H. H. Tye, *Physical Review A*, **30** (1984) 2005.

[4] M. C. de Sousa Vieira, E. Lazo, and C. Tsallis, *Physical Review A*, **35** (1987) 945.

[5] M. C. de Sousa Vieira and C. Tsallis, in *Universalities in Condensed Matter*, edited by R. Jullien, L. Peliti, R. Rammal, and N. Boccara (Springer-Verlag, New York, 1988).

[6] M. C. de Sousa Vieira and C. Tsallis, in *Disordered Systems and Biological Models*, edited by L. Peliti (World Scientific, Singapore, 1989).

[7] M. C. de Sousa Vieira and C. Tsallis, *Europhysics Letters*, **9** (1989) 119.

[8] M. C. de Sousa Vieira and C. Tsallis, *Physical Review A*, **40** (1989) 5305.

[9] M. C. de Sousa Vieira, *Physics Letters*, **143A** (1990) 279.

[10] M. G. Cosenza and J. B. Swift, *Physical Review A*, **43** (1991) 4095.

[11] V. Urumov, *Physics Letters*, **156A** (1991) 187.

[12] R. V. Jensen and L. K. H. Ma, *Physical Review A*, **31** (1985) 3993.

[13] T. T. Chia and B. L. Tan, *Physical Review A*, **44** (1991) R2231.

[14] T. T. Chia and B. L. Tan, *Physical Review A*, **45** (1992) 8441.

[15] B. L. Tan and T. T. Chia, *Physical Review E*, **47** (1993) 3087.

[16] B. L. Tan and T. T. Chia, *Physical Review E*, **52** (1995) 6885.

[17] W. M. Zheng, *Physical Review A*, **39** (1989) 6608.

[18] W. M. Zheng and L. S. Lu, *Communications in Theoretical Physics*, **15** (1991) 161.

[19] A. A. Hnilo, *Optics Communications*, **53** (1985) 194.

[20] A. A. Hnilo and M. C. de Sousa Vieira, *Journal of the Optical Society of America B*, **5** (1988) 928.

[21] M. Octovio, A. DaCosta, and J. Aponte, *Physical Review A*, **34** (1986) 1512.

[22] C. Marriott and C. Delisle, *Physica D*, **36** (1989) 198.

[23] K. Murali and M. Lakshmanan, *Physics Letters*, **151A** (1990) 412.

[24] K. Kaneko, *Collapse of Tori and Genesis of Chaos in Dissipative Systems* (World Scientific, Singapore, 1986).

[25] W. S. Ni, *Chinese Physics Letters*, **3** (1986) 573.

[26] A. L. Kawczynski and M. Misiurewicz, *Zeitschrift fur Physikalische Chemie* (Leipzig), **271** (1990) 1037.

[27] M. Misiurewicz and A. L. Kawczynski, *Physica D*, **52** (1991) 191.

[28] F. Aicardi and A. L. Kawczynski, *Complex Systems*, **6** (1992) 95.

[29] T. T. Chia and B. L. Tan, *Physical Review E*, **54** (1996) 5985.